Influence of artificial freezing on liquefaction characteristics of Nanjing sand

Jie Zhou and Zeyao Li
Department of Underground Building and Engineering, Tongji University, Shanghai, China, and
Wanjun Tian and Jiawei Sun
China Construction Second Engineering Bureau Co., LTD, Nanjing, China

Received 31 January 2023
Revised 12 February 2023
Accepted 12 February 2023

Abstract

Purpose – This study purposes to study the influence of artificial freezing on the liquefaction characteristics of Nanjing sand, as well as its mechanism.

Design/methodology/approach – was studied through dynamic triaxial tests by means of the GDS dynamic triaxial system on Nanjing sand extensively discovered in the middle and lower reaches of the Yangtze River under seismic load and metro train vibration load, respectively, and potential hazards of the two loads to the freezing construction of Nanjing sand were also identified in the tests.

Findings – The results show that under both seismic load and metro train vibration load, freeze-thaw cycles will significantly reduce the stiffness and liquefaction resistance of Nanjing sand, especially in the first freeze-thaw cycle; the more freeze-thaw cycles, the worse structural behaviors of silty-fine sand, and the easier to liquefy; freeze-thaw cycles will increase the sensitivity of Nanjing sand's dynamic pore pressure to dynamic load response; the lower the freezing temperature and the effective confining pressure, the worse the liquefaction resistance of Nanjing sand after freeze-thaw cycles; compared to the metro train vibration load, the seismic load in Nanjing is potentially less dangerous to freezing construction of Nanjing sand.

Originality/value – The research results are helpful to the construction of the artificial ground freezing of the subway crossing passage in the lower reaches of the Yangtze River and to ensure the construction safety of the subway tunnel and its crossing passage.

Keywords Metro, Foundation, Nanjing sand, Artificial formation freezing method, Sand liquefaction, Dynamic triaxial test

Paper type Research paper

1. Introduction

For the construction of underground space in coastal cities, the artificial strata freezing method can play the effect of soil layer reinforcement and efficient water isolation and sealing, which is commonly used for the construction of metro connected aisle and underground pump stations. Although the artificial strata freezing method is eco-friendly with advantages of good applicability and no pollution, the freezing effect will also change the physical and mechanical properties of soil (Mei, Zhao, Zhou, Liu, & Zhu, 2020), which may cause problems for tunnels and similar buildings, such as insufficient bearing capacity and increased deformation of the foundation.

The research was supported by the National Natural Science Foundation of China (Grant No. U41702299).

Railway Sciences
Vol. 2 No. 1, 2023
pp. 13-32
Emerald Publishing Limited
e-ISSN: 2755-0915
p-ISSN: 2755-0907
DOI 10.1108/RS-01-2023-0008

Saturated silty-fine sand is widely distributed along rivers (Huang, 2001) and is a soil layer commonly used by the artificial strata freezing method. At present, the dynamic characteristics of frozen and thawed saturated sand have been studied at home and abroad. For example, Yan, Wang, Liu, and Wang (2014) analyzed the influence of freeze-thaw cycles on the dynamic modulus and damping ratio of silty soil in the Naqu section of Qinghai–Tibet Railway. He, Wang, Liu, Jiang, and Liu (2017) analyzed the dynamic elastic modulus and damping ratio of undisturbed frozen soil and their relationship with vibration frequency and negative test temperature with the aid of a low-temperature dynamic triaxial tester in the context of seismic resistance of Qinghai–Tibet Railway. Based on the artificial strata freezing method, Tang, Li, and Li (2019) carried out the dynamic test of frozen and thawed saturated silt with the dynamic triaxial system and reached the conclusion that the axial strain is closely related to the dynamic pore water pressure, and the cumulative plastic deformation of silt can be significantly reduced by increasing the freezing temperature, vibration frequency and confining pressure and reducing the dynamic load amplitude. Johnson, Cole, and Chamberlain (1979), Sun, Gong, Xiong, and Gan (2020), Li, Baladi, and Andersland (1979) have also studied the dynamic elastic modulus and damping ratio of frozen and thawed soil. It can be seen that most studies on the dynamic characteristics of frozen and thawed saturated silty-fine sand at home and abroad focus on dynamic elastic modulus, damping ratio, stress–strain relationship, etc., and few focus on liquefaction characteristics.

Nanjing sand is a kind of saturated flaky silty-fine sand with liquefaction potential (Hu, Wang, Zhuang, & Chen, 2016) and is widely distributed in the lower reaches of the Yangtze River. Studying the influence of the freeze-thaw action on the liquefaction characteristics of Nanjing sand benefits the construction of metro connection aisles in the lower reaches of the Yangtze River by the artificial strata freezing method and helps ensure the construction and service safety of metro tunnels and their connection aisles.

In this paper, taking Nanjing sand as the research object, the water deposition-saturation-freezing-thawing device was used to prepare samples. Dynamic tests under two types of loads – seismic load and metro train vibration load – were performed with a GDS dynamic triaxial system to study the influence of the number of freeze-thaw cycles, freezing temperature and effective confining pressure on the liquefaction characteristics of Nanjing sand.

2. Test materials and sample preparation

2.1 Test materials

Taking the Nanjing sand near Shang Yuanmen metro station in Gulou District, Nanjing, as the research object, its sand layer belongs to a water environment deposit layer typical on a flood plain (Huang, 2001). This area has high underground water level with saturated sand layer and medium density. The grain gradation and shape of Nanjing sand are shown in Figure 1. Its major component is quartz clasts with a laminated structure and anisotropy, which is more prone to liquefaction than ordinary round sand grains (Chen, Sun, Liu, Hu, & Zeng, 2003). See Table 1 for basic physical properties.

2.2 Sample preparation

The Nanjing sand used in the test is structurally strong and relatively loose, and in order to ensure the structural arrangement of flaky grains, it is remolded and prepared by sand raining method. The undisturbed samples are dried, sieved and then prepared. The sample preparation device for the sand raining method is as shown in Figure 2, which consists of a sanding device with adjustable drop distance and amount, a water tank, a movable trolley platform and a double valve for sand loading. The water level in the tank is 1 m above the

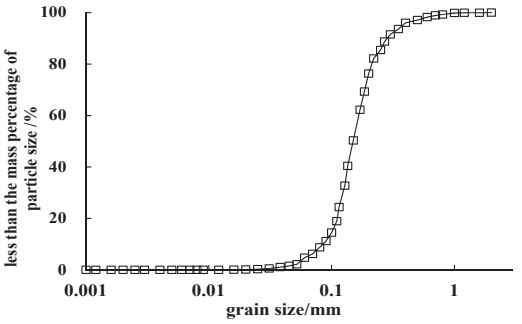

Grain gradation

(a)

Grain shape

(b)

Figure 1.
Grain characteristics of Nanjing sand

Mean grain size, d_{50}/mm	Non-uniformity coefficient, C_u	Specific gravity of soil grains, $G_S/(g \cdot cm^{-3})$	Natural void ratio, e	Maximum void ratio, e_{max}	Minimum void ratio, e_{min}	Effective internal friction angle, $\varphi'/(°)$	Cohesion, c/kPa
0.16	2.13	2.67	0.897	1.13	0.65	27.3	3.1

Table 1.
Basic physical properties of Nanjing sand

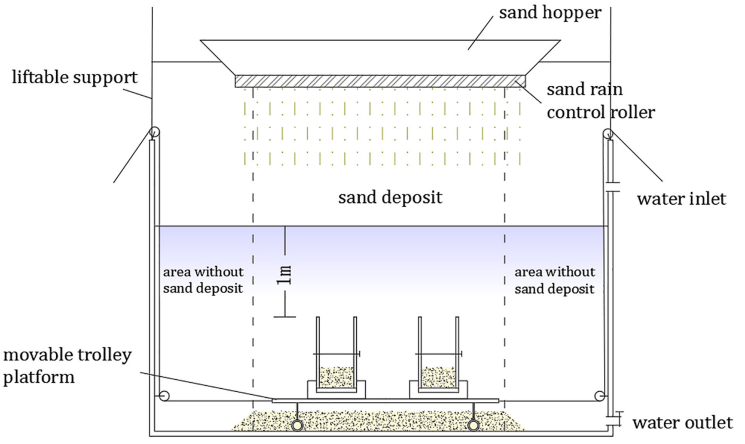

Figure 2.
Schematic diagram of sample preparation device by sand raining method

height of the sand sample (Lagioia, Sanzeni, & Colleselli, 2006; Wang, Wang, & Li, 2004). The movable trolley platform is specially designed and manufactured to avoid sorting among the first deposited sand due to different fall rates of coarse and fine sand at the beginning of sanding (Cheng, Wang, & Li, 2016). After a period of time (30 s) of sanding, the trolley is moved to the sand deposit to collect sand. The density of sand samples can be controlled roughly by regulating the drop distance and amount and then that of the soil samples can be controlled accurately by using a sample presser. The sample has a grain size of 39.1 mm and a height of 80 mm. After compaction, the sand sample is saturated in a vacuum saturator for 12 h.

After saturation, samples without the need for freezing and thawing can be moved directly to a dynamic triaxial tester. For samples to be frozen and thawed, first, place them into a freeze-thaw device (as shown in Figure 3) for pre-compaction, which is performed by opening the drain and loading appropriate weight blocks to compact the sand sample. The load provided by weights shall match the axial pressure of the sample intended for triaxial test. Next, close the drainage channel after 2 h of preloading, and put the freeze-thaw device together with the weights into a DW-40 low-temperature test chamber for 24 h of freezing (Tang *et al.*, 2019). Then, after the completion of freezing, remove the protective mold immediately, place the sample on the dynamic triaxial tester, apply the confining pressure and wait for thawing. Finally, after thawing for 24 h and the strain of the soil sample no longer increases, apply a vibration load to the sand sample for undrained dynamic triaxial test.

3. Test schemes

Metro tunnels and their connection aisles in coastal areas have an average depth of 10–15 m, and the average temperature of the frozen curtain is −15 °C when the artificial strata freezing method is adopted (Tang *et al.*, 2019). In most working conditions, the strata is required to be frozen only once, and in very few working conditions, freezing for the second time may be required due to internal project reasons to make up for the problems caused by the first

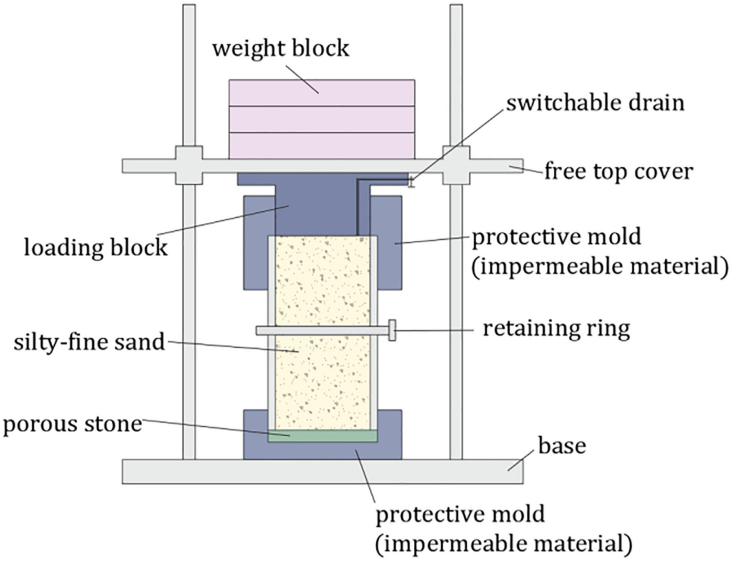

Figure 3.
Schematic diagram of the freeze-thaw device

freezing. This paper considers only the conditions of one or two freeze-thaw cycles, and excludes the condition of more freeze-thaw cycles.

3.1 Test scheme under seismic load

Earthquakes feature characteristics of suddenness, briefness and high amplitude, and the test simulates an earthquake by exciting unidirectional sine waves. The influences of the number of freeze-thaw cycles, freezing temperature and effective confining pressure on the liquefaction characteristics of Nanjing sand are tested based on the working conditions of a 12.5 m deep tunnel, i.e. confining pressure of 250 kPa, back pressure of 125 kPa, freezing temperature of −15 °C, dynamic load vibration frequency of 1 Hz and one freeze-thaw cycle. The liquefaction failure criterion is up to 5% double-amplitude strain (Lagioia *et al.*, 2006). See Table 2 for the test scheme.

The simulated earthquake load is constant sinusoidal load. Taking A4 sample as an example, the time history curve of its dynamic load is shown in Figure 4.

3.2 Test scheme under metro train vibration load

The metro train vibration load has a low amplitude, but a long action time. Since the metro train itself has its own dead weight, the vibration load from the metro train can be simulated as the reference dynamic load plus its amplitude. According to field data (Zhang, 2016), the vibration frequency of soil around a tunnel is 0.2–2.0 Hz when a metro train is running, the reference value of metro train vibration load is about 30 kPa, and the amplitude of dynamic load is 10–20 kPa. Unidirectional excitation and isotropic consolidation are adopted in the test. The influences of the number of freeze-thaw cycles, freezing temperature, vibration frequency and effective confining pressure on the liquefaction characteristics of Nanjing sand are tested based on the working conditions of a 12.5 m deep tunnel, i.e. confining pressure of 250 kPa, back pressure of 125 kPa, freezing temperature of −15 °C, vibration frequency of 1 Hz, reference dynamic load of 30 kPa, dynamic load amplitude of 15 kPa and one freeze-thaw cycle. The liquefaction failure criterion is whether the double-amplitude strain reaches 5% (Hu *et al.*, 2016). See Table 3 for the test scheme.

After the test starts, the reference dynamic load is applied within 2s. Figure 5 shows the time history curve of dynamic load on D4.

4. Test results under seismic load condition

4.1 Influence of freeze-thaw cycles on development law of strain and dynamic pore pressure in Nanjing sand

A total of nine tests numbered A1–A9 were carried out under seismic load conditions to analyze the influence of freeze-thaw cycles on the development law of strain and dynamic pore pressure in Nanjing sand. Figure 6–8 show the test results under the seismic load condition with confining pressure of 250 kPa, freezing temperature of −15 °C and dynamic load amplitude of 75 kPa. Figure 6 shows the time history curves of axial strain in Nanjing sand subjected to no freeze-thaw cycle (A1), one freeze-thaw cycle (A4) and two freeze-thaw cycles (A7). It can be seen from Figure 6 that the number of vibrations for Nanjing sand to liquefy is 35, 24 and 22, respectively, in cases of no freeze-thaw cycle, one freeze-thaw cycle and two freeze-thaw cycles; it is easier to liquefy frozen and thawed Nanjing sand, and the more freeze-thaw cycles, the easier to liquefy, but the first freeze-thaw cycle has the greatest impact; given the same number of vibrations, the dynamic strain (axial strain) is the smallest in sand subjected to no freeze-thaw cycle, and it increases obviously with one freeze-thaw cycle and further increases slightly with two freeze-thaw cycles, indicating that freeze-thaw cycles can reduce the stiffness of Nanjing sand; under the same number of vibrations, the

Table 2.
Test scheme under seismic load

Sample no.	Simulated depth/m	Axial pressure/kPa	Confining pressure/kPa	Back pressure/kPa	Freezing temperature/°C	Dynamic load amplitude/kPa	Vibration frequency/Hz	Number of freeze-thaw cycles
A1	12.5	250	250	125	−15	75	1.0	0
A2	12.5	250	250	125	−15	50	1.0	0
A3	12.5	250	250	125	−15	100	1.0	0
A4	12.5	250	250	125	−15	75	1.0	1
A5	12.5	250	250	125	−15	50	1.0	1
A6	12.5	250	250	125	−15	100	1.0	1
A7	12.5	250	250	125	−15	75	1.0	2
A8	12.5	250	250	125	−15	50	1.0	2
A9	12.5	250	250	125	−15	100	1.0	2
B1	12.5	250	250	125	−5	75	1.0	1
B2	12.5	250	250	125	−5	50	1.0	1
B3	12.5	250	250	125	−5	100	1.0	1
B4	12.5	250	250	125	−25	75	1.0	1
B5	12.5	250	250	125	−25	50	1.0	1
B6	12.5	250	250	125	−25	100	1.0	1
C1	10.0	200	200	100	−15	75	1.0	1
C2	10.0	200	200	100	−15	50	1.0	1
C3	10.0	200	200	100	−15	100	1.0	1
C4	15.0	300	300	150	−15	75	1.0	1
C5	15.0	300	300	150	−15	50	1.0	1
C6	15.0	300	300	150	−15	100	1.0	1

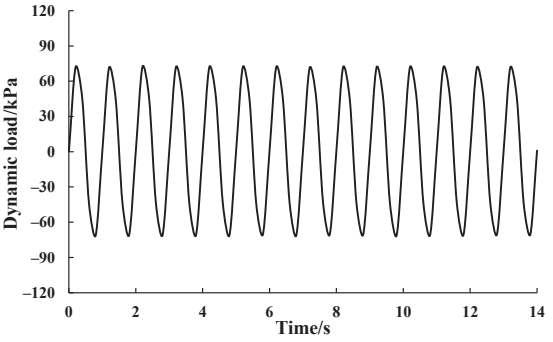

Figure 4.
Time history curve of dynamic load on A4

cumulative plastic deformation increases with the increase in the number of freeze-thaw cycles, and Nanjing sand subjected to freezing and thawing is more likely to occur plastic deformation.

Figure 7 shows the time history curves of dynamic pore pressure in Nanjing sand subjected to no freeze-thaw cycle (A1), one freeze-thaw cycle (A4) and two freeze-thaw cycles (A7). The growth curve of the dynamic pore pressure ratio of Nanjing sand is roughly divided into three stages:

(1) the initial stage, in which the average dynamic pore pressure ratio increases rapidly under one vibration and continues to increase as the number of vibrations increases but at a gradually decreasing rate, and the growth amplitude increases rapidly;

(2) the steady growth stage, in which both the average dynamic pore pressure ratio and the growth amplitude increase steadily under one vibration at a basically constant rate;

(3) the near-liquefaction stage, after the dynamic pore pressure ratio comes to about 0.92, in which the maximum dynamic pore pressure ratio will maintain at about 0.95, the minimum will rise sharply until complete liquefaction, and the more vibrations, the longer the maximum dynamic pore pressure ratio remains the same under one vibration. Given the same number of vibrations in the test process, both the average and amplitude of the dynamic pore pressure ratio of Nanjing sand are the smallest in the case of no freeze-thaw cycle, and the values are obviously larger in samples through one freeze-thaw cycle than those without freeze-thaw cycle and slightly lower than those frozen and thawed twice. It can be seen that the freeze-thaw action can increase the sensitivity of dynamic pore pressure in response to dynamic load.

Figure 8 shows the hysteretic curves of Nanjing sand subjected to no freeze-thaw cycle (A1), one freeze-thaw cycle (A4) and two freeze-thaw cycles (A7). It can be seen from Figure 8 that the more vibrations, the more significant the asymmetry of the hysteretic curve regardless of whether the Nanjing sand is subjected to freezing and thawing. Ma, Chen, Li, Wu, and Liu (2019) proposed to express the energy dissipation of soil mass in the hysteresis loop area and add all energy dissipation in the loading process to obtain the total energy required to liquefy the soil mass. The calculated total energy dissipation of Nanjing sand is 1,271kJ$\cdot$m^{-3}, 977 kJ$\cdot$m^{-3} and 894 kJ$\cdot$m^{-3}, respectively, in the cases of no freeze-thaw cycle, one freeze-thaw cycle and two freeze-thaw cycles. It indicates that Nanjing sand subjected to freezing and thawing consumes less energy for liquefaction, has poor structural behaviors and is more likely to be damaged.

Table 3.
Test scheme under metro train vibration load

Sample no.	Simulated depth/m	Axial pressure/kPa	Confining pressure/kPa	Back pressure/kPa	Freezing temperature/°C	Dynamic load amplitude/kPa	Vibration frequency/Hz	Number of freeze-thaw cycles
D1	12.5	250 + 30	250	125	−15	15	1.0	0
D2	12.5	250 + 30	250	125	−15	10	1.0	0
D3	12.5	250 + 30	250	125	−15	20	1.0	0
D4	12.5	250 + 30	250	125	−15	15	1.0	1
D5	12.5	250 + 30	250	125	−15	10	1.0	1
D6	12.5	250 + 30	250	125	−15	20	1.0	1
D7	12.5	250 + 30	250	125	−15	15	1.0	2
D8	12.5	250 + 30	250	125	−15	10	1.0	2
D9	12.5	250 + 30	250	125	−15	20	1.0	2
E1	12.5	250 + 30	250	125	−5	15	1.0	1
E2	12.5	250 + 30	250	125	−5	10	1.0	1
E3	12.5	250 + 30	250	125	−5	20	1.0	1
E4	12.5	250 + 30	250	125	−25	15	1.0	1
E5	12.5	250 + 30	250	125	−25	10	1.0	1
E6	12.5	250 + 30	250	125	−25	20	1.0	1
F1	12.5	250 + 30	250	125	−15	15	0.2	1
F2	12.5	250 + 30	250	125	−15	10	0.2	1
F3	12.5	250 + 30	250	125	−15	20	0.2	1
F4	12.5	250 + 30	250	125	−15	15	0.5	1
F5	12.5	250 + 30	250	125	−15	10	0.5	1
F6	12.5	250 + 30	250	125	−15	20	0.5	1
F7	12.5	250 + 30	250	125	−15	15	2.0	1
F8	12.5	250 + 30	250	125	−15	10	2.0	1
F9	12.5	250 + 30	250	125	−15	20	2.0	1
G1	10.0	200 + 30	200	100	−15	15	1.0	1
G2	10.0	200 + 30	200	100	−15	10	1.0	1
G3	10.0	200 + 30	200	100	−15	20	1.0	1
G4	15.0	300 + 30	300	150	−15	15	1.0	1
G5	15.0	300 + 30	300	150	−15	10	1.0	1
G6	15.0	300 + 30	300	150	−15	20	1.0	1

4.2 Influence of number of freeze-thaw cycles on liquefaction characteristics of Nanjing sand

The cyclic stress ratio C_{SR} is usually used to measure the liquefaction characteristics of saturated sand liquefaction tested. Under isotropic consolidation condition, the cyclic stress ratio C_{SR} is the ratio of the cyclic shear stress amplitude on the plane of a sand sample suffering the maximum cyclic shear stress τ_d to the effective confining pressure p', (Ma *et al.*, 2019).

$$C_{SR} = \frac{\tau_d}{p'} = \frac{\sigma_d}{2p'} \quad (1)$$

where σ_d is the dynamic load amplitude in kPa.

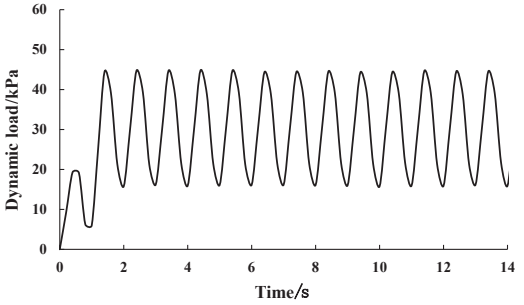

Figure 5.
Time history curve of dynamic load on D4

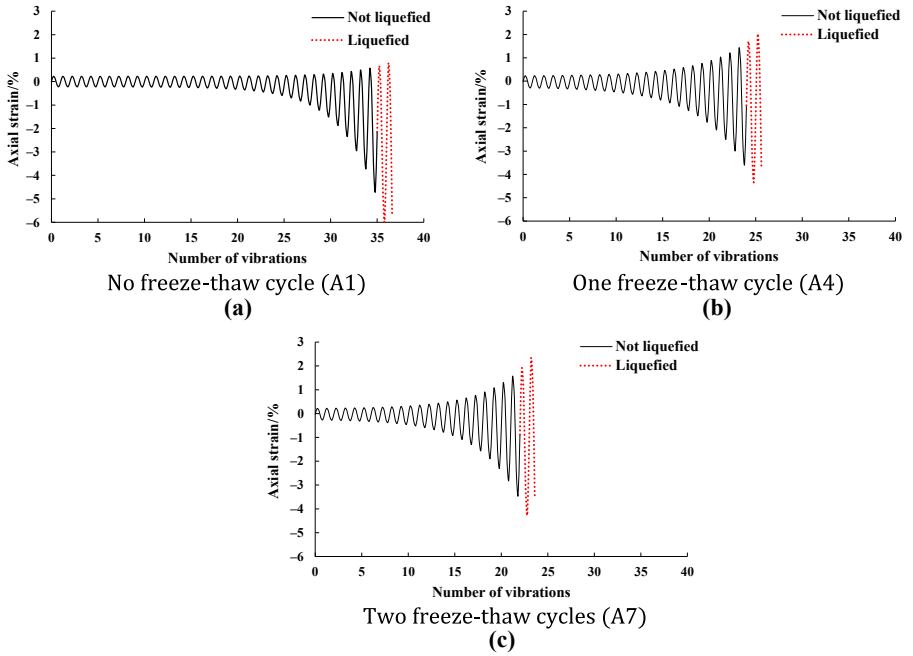

Figure 6.
Time history curve of strain in Nanjing sand under seismic load condition

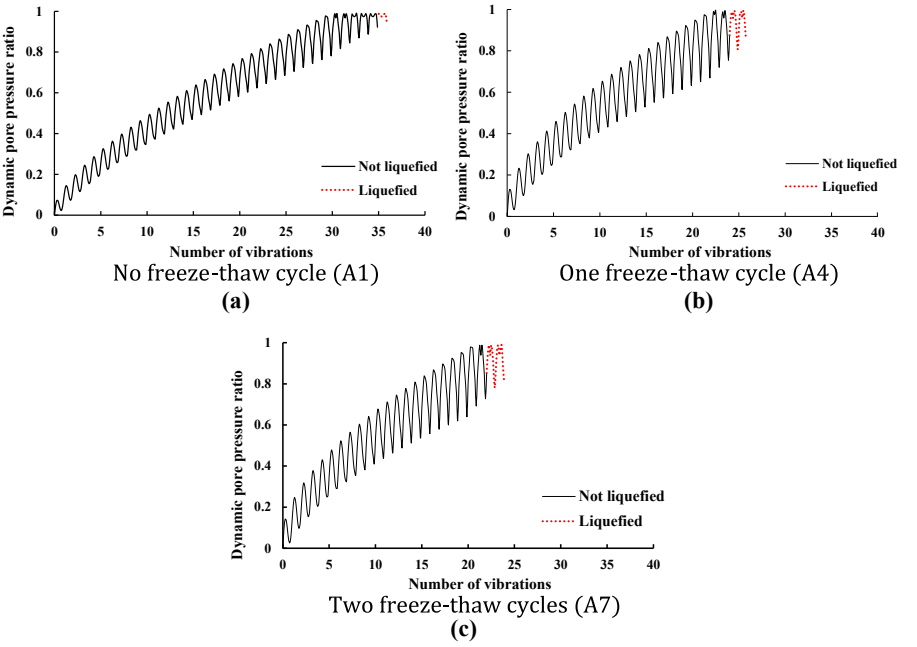

Figure 7.
Time history curve of dynamic pore pressure in Nanjing sand under seismic load condition

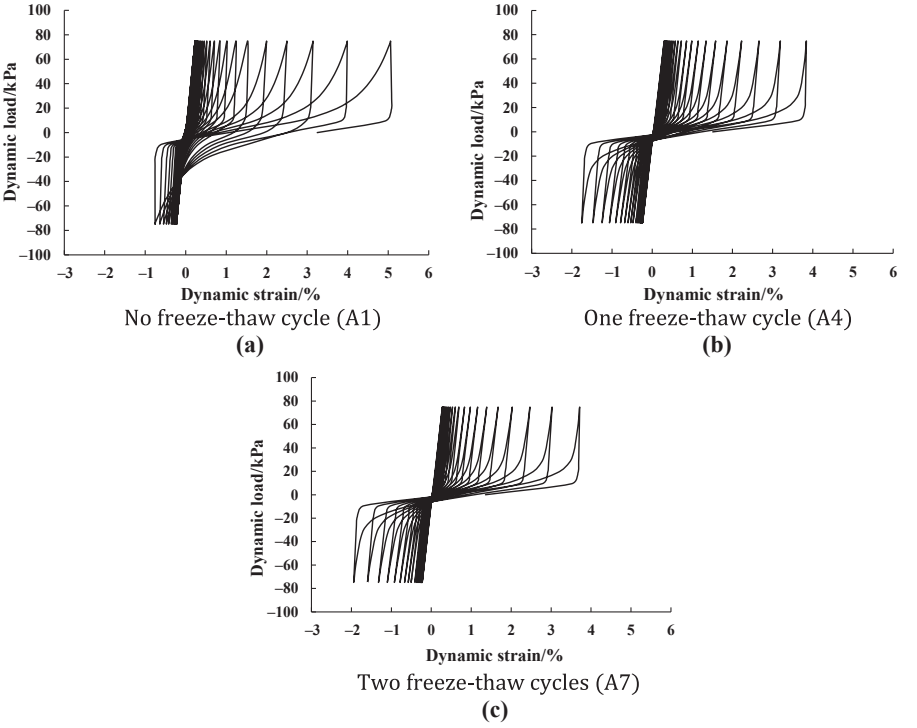

Figure 8.
Hysteretic curve of Nanjing sand under seismic load condition

Figure 9 shows the relationship between the number of freeze-thaw cycles and the number of liquefaction cycles of Nanjing sand under seismic load with different cyclic stress ratios. It can be seen from Figure 9 that when the number of freeze-thaw cycles is not greater than two and the same, the larger the cyclic stress ratio, the fewer liquefaction cycles, that is, the more liable it is for Nanjing sand to liquefy, and that when the cyclic stress ratio of the seismic load is the same, the number of liquefaction cycles of Nanjing sand decreases with the increasing number of freeze-thaw cycles. This indicates that the freeze-thaw cycle can weaken the liquefaction resistance of Nanjing sand, and there is a significant decline in the liquefaction resistance of Nanjing sand after freezing and thawing.

4.3 Influence of freezing temperature on liquefaction characteristics of Nanjing sand

Figure 10 shows the relationship between the freezing temperature and the number of liquefaction cycles of Nanjing sand under seismic load with different cyclic stress ratios. It can be seen from Figure 10 that the freezing temperature is in the range of −25 – −5 °C, and the number of liquefaction cycles of Nanjing sand under seismic load with the same cyclic stress ratio decreases with the dropping freezing temperature. This indicates that the lower the freezing temperature, the easier it is to liquefy Nanjing sand subjected to freezing and thawing.

4.4 Influence of effective confining pressure on liquefaction characteristics of Nanjing sand

Figure 11 shows the relationship between the effective confining pressure and the number of liquefaction cycles of Nanjing sand under seismic load with different cyclic stress ratios. It can be seen from Figure 11 that the effective confining pressure is within the range of 100−150 kPa, and the smaller the effective confining pressure, the fewer liquefaction cycles of Nanjing sand subjected to freezing and thawing under the seismic load with the same cyclic

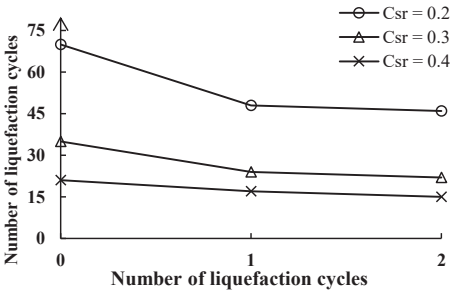

Figure 9.
Number of liquefaction cycles vs number of freeze-thaw cycles (seismic load)

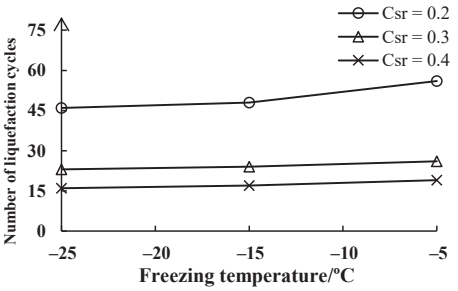

Figure 10.
Number of liquefaction cycles vs freezing temperature (seismic load)

stress ratio. This indicates that the smaller the effective confining pressure, the easier the liquefaction of such Nanjing sand.

4.5 Liquefaction evaluation of Nanjing sand under seismic load condition

Huang (2001) studied the liquefaction characteristics of Nanjing sand and found that Seed's simplified procedure for evaluating soil liquefaction potential is effective in establishing the seismic liquefaction characteristics of Nanjing sand.

In Seed's simplified procedure, whether soil mass is liquefied is judged by comparing the magnitude of seismic shear stress at different depths on the site τ_E and of liquefaction strength of sand under seismic load τ_s. The seismic shear stress τ_E at a depth of d_s can be calculated by the formula below.

$$\tau_E = 0.65 a_{max} \frac{K \gamma d_s}{g} \tag{2}$$

and

$$K = \begin{cases} 1 - 0.01 d_s & d_s < 10 \\ 1.2 - 0.03 d_s & d_s \geq 10 \end{cases}$$

where a_{max} is the peak ground acceleration, in $m \cdot s^{-2}$; γ is the natural unit weight of overlaying soil, in $kN \cdot m^{-3}$; g is the gravity acceleration, in $m \cdot s^{-2}$; K is the depth reduction coefficient (Chen *et al.*, 2003).

The liquefaction resistance shear stress of the sand layer τ_s can be calculated by the formula below (Huang, 2001).

$$\tau_s = C_r C_{RR} p' \tag{3}$$

where C_r is the coefficient of stress difference in the dynamic triaxial test, which is suggested in the reference (Wang *et al.*, 2004) to take 0.65; C_{RR} is the liquefaction resistance in the dynamic triaxial test.

Depending on the seismic risk of the area in question, C_{RR} can be expressed by C_{SR}, the number of load cycles until liquefaction (Huang, 2001; Zhang, 2016). Taking Nanjing City, whose seismic intensity is VII and design basic acceleration of ground motion is 0.1 g, as an example, C_{RR} takes the value of C_{SR}, i.e. 12 load cycles until Nanjing sand liquefies.

The results of the dynamic triaxial test show that sand within the depth range of Nanjing metro connection aisles (10-15 m) cannot liquefy after 12 vibrations even if it is subjected to two freeze-thaw cycles. See Table 4 for the liquefaction evaluation results of Nanjing sand at a depth of 12.5 m.

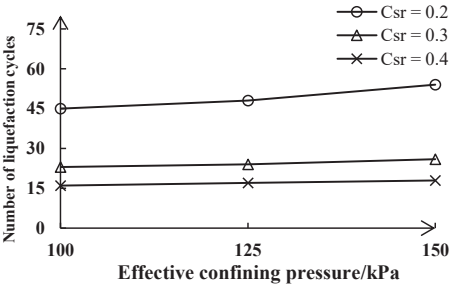

Figure 11.
Number of liquefaction cycles vs effective confining pressure (seismic load)

It can be seen from Table 4 that the freeze-thaw cycle can reduce the liquefaction resistance of Nanjing sand. In Nanjing, artificial freezing and thawing of Nanjing sand will not trigger liquefaction under an M7 earthquake with 0.1 *g* acceleration. This indicates that the seismic load poses a low potential risk to Nanjing sand freezing construction.

5. Test results under metro train vibration load condition

5.1 Influence of freeze-thaw cycles on development law of strain and dynamic pore pressure in Nanjing sand

A total of nine tests numbered D1–D9 were carried out under metro train vibration load condition to analyze the influence of freeze-thaw cycles on the development law of strain and dynamic pore pressure in Nanjing sand. Figure 12–14 show the test results under the metro train vibration load condition with effective confining pressure of 125 kPa, freezing temperature of −15 ℃, reference dynamic load of 30 kPa, dynamic load amplitude of 15 kPa, and vibration frequency of 1 Hz. Figure 12 shows the time history curves of strain in Nanjing sand subjected to no freeze-thaw cycle (D1), one freeze-thaw cycle (D4) and two freeze-thaw cycles (D7). It can be seen from Figure 12 that the number of vibrations required for

Number of freeze-thaw cycles	Freezing temperature/℃	τ_E/kPa	τ_s/kPa	τ_s/τ_E	Liquefied or not
0	−15	13.40	39.49	2.87	no
1	−15	13.40	36.53	2.73	no
2	−15	13.40	34.48	2.57	no
1	−5	13.40	37.45	2.79	no
1	−25	13.40	35.79	2.67	no

Table 4. Liquefaction evaluation results under seismic load

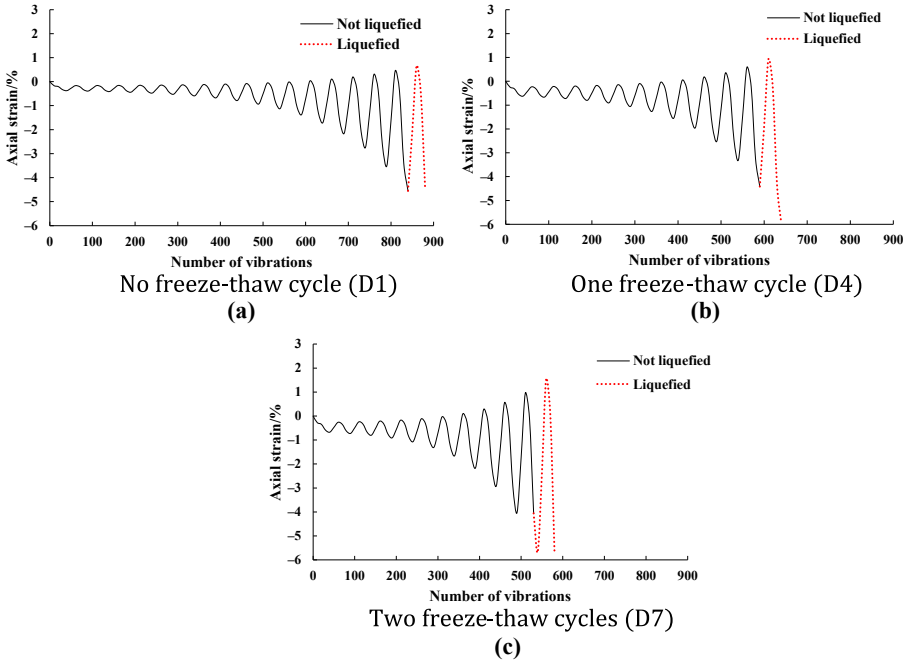

Figure 12. Time history curve of strain in Nanjing sand under metro train vibration condition

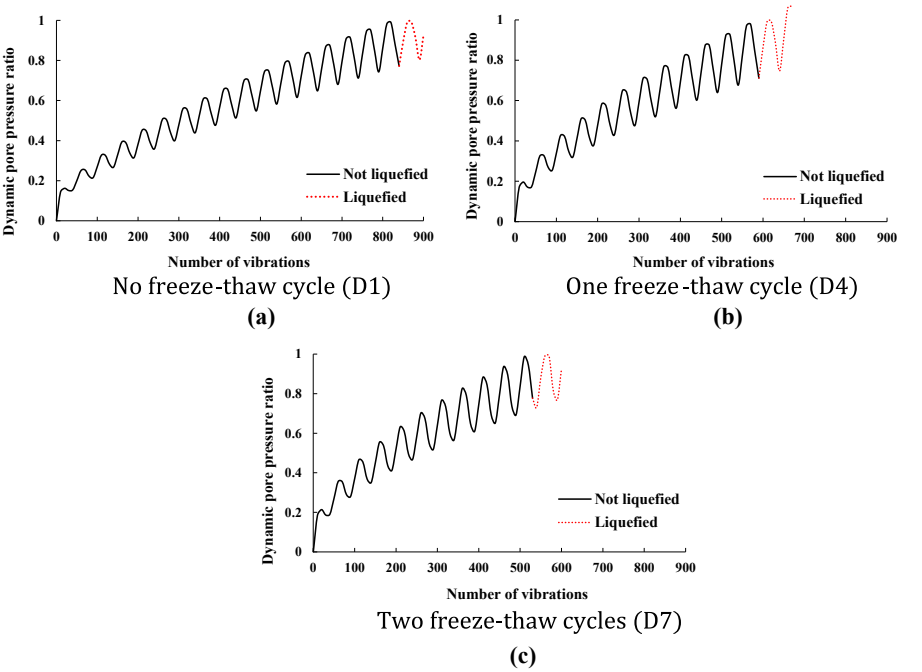

Figure 13.
Time history curve of dynamic pore pressure in Nanjing sand under metro train vibration condition

liquefaction of Nanjing sand subjected to no freeze-thaw cycle, one freeze-thaw cycle and two freeze-thaw cycles is 841, 594 and 528, respectively; due to the reference dynamic load, Nanjing sand has an initial strain of about 0.2% at the beginning of vibration; similar to phenomena in the test under seismic load, Nanjing sand subjected to freezing and thawing is more likely to liquefy under metro train vibration load, and the more freeze-thaw cycles, the easier; the first freeze-thaw cycle has the greatest impact; Nanjing sand subjected to freezing and thawing is less rigid and more prone to plastic deformation.

Figure 13 shows the time history curves of dynamic pore pressure in Nanjing sand subjected to no freeze-thaw cycle (D1), one freeze-thaw cycle (D4) and two freeze-thaw cycles (D7). It can be seen from Figure 13 that the development of dynamic pore pressure in Nanjing sand before liquefaction is roughly similar to that in the seismic load condition, but the minimum pore pressure ratio will still rise slowly after the soil mass reaches the liquefaction condition. The slow rather than rapid rise indicates that Nanjing sand still has strength in a short time after it liquefies under metro train vibration load.

Figure 14 shows the hysteretic curves of dynamic load and axial strain of Nanjing sand subjected to no freeze-thaw cycle (D1), one freeze-thaw cycle (D4) and two freeze-thaw cycles (D7). It can be seen from Figure 14 that under metro train vibration load, the total energy required for liquefaction of Nanjing sand subjected to no freeze-thaw cycle, one freeze-thaw cycle and two freeze-thaw cycles is 1,189,929 and 857 $kJ \cdot m^{-3}$, respectively. This indicates that the more freeze-thaw cycles, the less energy required for liquefaction, the worse structure and the more liable to damage.

5.2 Influence of number of freeze-thaw cycles on liquefaction characteristics of Nanjing sand

Figure 15 shows the relationship between the number of liquefaction cycles and the number of freeze-thaw cycles of Nanjing sand under metro train vibration loads with different cyclic

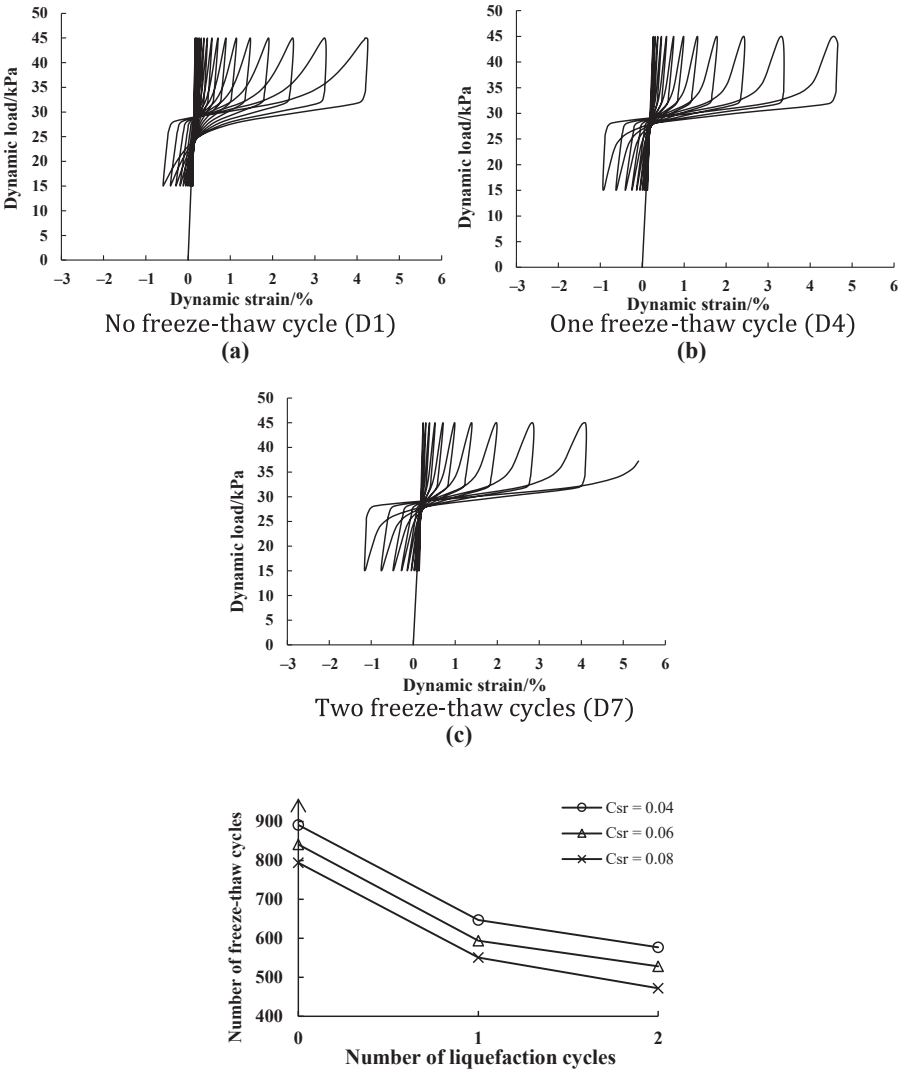

Figure 14.
Hysteretic curve of Nanjing sand under metro train vibration condition

Figure 15.
Number of liquefaction cycles vs number of freeze-thaw cycles (metro train vibration load)

stress ratios. It can be seen that the number of liquefaction cycles of Nanjing sand decreases with the increase in the number of freeze-thaw cycles, which is most conspicuous with the first freeze-thaw cycle, provided the cyclic stress ratio of the metro train vibration load is the same and it undergoes no more than two freeze-thaw cycles. This indicates that freeze-thaw cycles can weaken the liquefaction resistance of Nanjing sand, especially the first freeze-thaw cycle with the largest influence.

5.3 Influence of freezing temperature on liquefaction characteristics of Nanjing sand

Figure 16 shows the relationship between the number of liquefaction cycles and the freezing temperature of Nanjing sand under metro train vibration loads with different cyclic stress ratios. It can be seen from Figure 16 that the freezing temperature is in the range of −25 – −5 °C,

and the number of liquefaction cycles of Nanjing sand under metro train vibration load with the same cyclic stress ratio decreases with the dropping freezing temperature. This indicates that the lower the freezing temperature, the easier it is to liquefy Nanjing sand subjected to freezing and thawing.

5.4 Influence of vibration frequency on liquefaction characteristics of Nanjing sand

Figure 17 shows the relationship between the vibration frequency and the number of liquefaction cycles of Nanjing sand under metro train vibration loads with different cyclic stress ratios. As can be seen, the vibration frequency is in the range of 0.2–2.0 Hz, and the number of liquefaction cycles of Nanjing sand decreases with its increase under the metro train vibration load with the same cyclic stress ratio. This indicates that high-frequency vibration is more likely to trigger the liquefaction of Nanjing sand subjected to freezing and thawing.

5.5 Influence of effective confining pressure on liquefaction characteristics of Nanjing sand

Figure 18 shows the relationship between the effective confining pressure and the number of liquefaction cycles of Nanjing sand under metro train vibration load with different cyclic stress ratios.

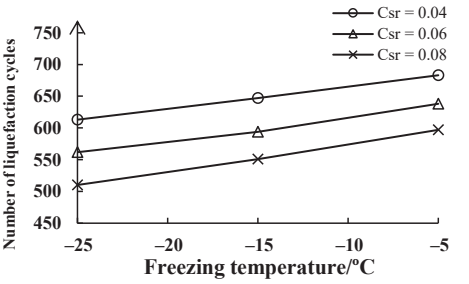

Figure 16.
Number of liquefaction cycles vs freezing temperature (metro train vibration load)

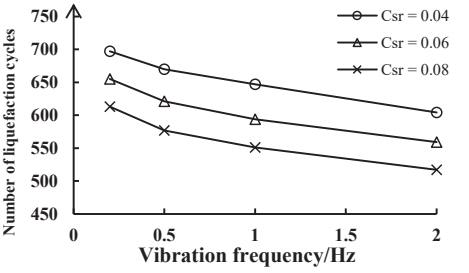

Figure 17.
Number of liquefaction cycles vs vibration frequency (metro train vibration load)

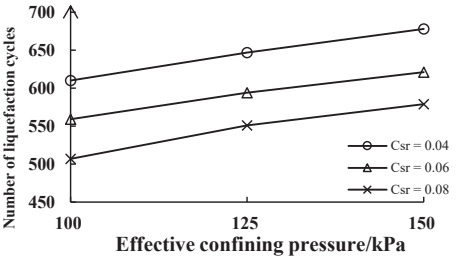

Figure 18.
Number of liquefaction cycles vs effective confining pressure (metro train vibration load)

As can be seen, the effective confining pressure is within the range of 100–150 kPa, and the smaller the effective confining pressure, the fewer liquefaction cycles, under the same cyclic stress ratio of the metro train vibration load. This indicates that smaller effective confining pressures make it easier to liquefy Nanjing sand subjected to freezing and thawing.

5.6 Suggestions on liquefaction evaluation of Nanjing sand under metro train vibration load

Unlike the seismic load that lasts for tens of seconds, the metro train vibration load will last for more than ten hours intermittently, and the number of vibrations from metro trains can reach tens of thousands each day. If the water permeability of the sand layer is insufficient or the drainage channel is not smooth, the metro train vibration load may cause the liquefaction of Nanjing sand. For Nanjing sand, the artificial formation freezing method can raise the possibility of its liquefaction, and its liquefaction would be easier with more freeze-thaw cycles and lower freezing temperatures.

The following engineering suggestions are put forward in consideration of the influence of freezing and thawing on the liquefaction of Nanjing sand under the metro train vibration load:

(1) The freezing effect will enhance the possibility of liquefaction of Nanjing sand, and thus in areas with liquefaction potential, evaluation and treatment should be carried out for Nanjing sand each time after freezing construction;

(2) If the water permeability of the sand layer is insufficient, or the metro is surrounded with diaphragm walls and other water-resisting structures, Nanjing sand shall be treated for better liquefaction resistance, and all efforts shall be made to ensure smooth drainage in surroundings of metro construction.

6. Freeze-thaw characteristics and liquefaction mechanism of Nanjing sand

6.1 Freeze-thaw characteristics

Nanjing sand is subject to frost heaves and thaw settlement under certain conditions. After freezing, the frost heave rate of Nanjing sand can be obtained by measuring the sample with a vernier caliper. After the sample is melted on a dynamic triaxial tester, the melt sinking rate of Nanjing sand can be obtained according to the strain monitoring results of the dynamic triaxial test (Coal Industry Coal Mine Special Equipment Standardization Technical Committee, 2011). Table 5 gives the freeze-thaw characteristics of samples under different

Freezing condition	Test number	Frost heaving rate/%	Thaw settlement rate/%
Freezing temperature: 15 °C; effective confining pressure: 125 kPa; one freeze-thaw cycle	A4—A6 D4—D6 F1—F9	3.31	3.69
Freezing temperature: 5 °C; effective confining pressure: 125 kPa; one freeze-thaw cycle	B1—B3 E1—E3	3.25	3.61
Freezing temperature: 25 °C; effective confining pressure: 125 kPa; one freeze-thaw cycle	B4—B6 E4—E6	3.43	3.80
Freezing temperature: 15 °C; effective confining pressure: 100 kPa; one freeze-thaw cycle	C1—C3 G1—G3	3.37	3.73
Freezing temperature: 15 °C; effective confining pressure: 150 kPa; one freeze-thaw cycle	C4—C6 G4—G6	3.28	3.62
Freezing temperature: 15 °C; effective confining pressure: 125 kPa; two freeze-thaw cycles	A7—A9 D7—D9	3.29	3.71

Table 5. Freeze-thaw characteristics of Nanjing sand

freezing temperatures, effective confining pressures and numbers of freeze-thaw cycles. The effective confining pressure is the difference between the confining pressure and the back pressure.

As the table shows, the frost heave rate of Nanjing sand is about 3.3%, and its thaw settlement rate is about 3.7%. After one freeze-thaw cycle, the sample volume decreases by about 0.5% and the void ratio decreases. After two freeze-thaw cycles, the sample will also undergo frost heave and thaw settlement, and the void ratio will further decrease.

Compared with the frost heave and thaw settlement rates (5%–7%) of silt and clay (Wang, Xu, Liu, Wang, & Liu, 2016), the frost heave and thaw settlement rates of Nanjing silty-fine sand are relatively small. This is due to the relatively small capillary water content of silty-fine sand, which makes strong segregation and frost heave impossible. Larger confining pressures and higher freezing temperatures will reduce frost heaves and thaw settlement. However, in general, the frost heave and thaw settlement rates of Nanjing silty-fine sand change little when the confining pressure, freezing temperature or freezing count in the scope of artificial formation freezing changes. The effective confining pressure, freezing temperature and freezing count all have a slight influence on the frost heave and thaw settlement characteristics of Nanjing silty-fine sand.

6.2 Influence mechanism of freeze-thaw action on liquefaction characteristics

Freeze-thaw action will affect the grain and pore characteristics of soil mass and thereby its liquefaction response. Liquefaction failure occurred after the sample was thawed and vibrated on the dynamic triaxial tester, and the grain and pore characteristics could not be measured in time. Therefore, a new sample was frozen and thawed in the freezer, and the grain characteristics of the frozen and thawed sample were determined, as shown in Table 6. It can be seen that the grain size of Nanjing sand is smaller with more freeze-thaw cycles.

The pore characteristics of frozen, thawed and then air-dried Nanjing silty-fine sand were determined with a mercury intrusion tester, as shown in Figure 19. It can be seen that

Table 6.
Gradation of Nanjing sand after frost heave and thaw settlement tests

Particle size/mm	Accumulative percentage of residues/%		
	Not frozen	One freeze-thaw cycle	Two freeze-thaw cycles
<0.005	0.2	0.3	0.4
<0.050	2.5	2.6	2.6
<0.075	14.3	14.9	15.2
<0.100	85.8	86.6	87.1
<0.500	96.1	96.2	96.2
<1.000	100.0	100.0	100.0

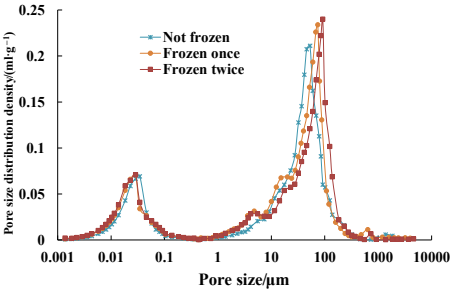

Figure 19.
Pore characteristics of frozen and thawed sand

the pore size of Nanjing sand is mainly distributed in the range of 10–100 μm and freezing and thawing can increase the size and count of large pores and reduce the size of small pores.

During the freezing process of soil mass, free water in the large pores first undergoes a phase change and volume expansion, resulting in frost heave force (Mei *et al.*, 2020; Wang *et al.*, 2016). The frost heave force expands the large pores and squeezes the sand grains and small pores containing unfrozen water, breaking the grains, shrinking the small pores (Wang, Wang, Song, Wang, & Liu, 2019), and destroying the structure of the soil itself. After thawing, the influence of freezing on pores and the structure of sandy soil cannot be completely eliminated, and thus it was found that the grain size of frozen-thawed Nanjing sand decreases, large pore sizes increase and small pore sizes decrease. Decreasing grain sizes and increasing large pore sizes make it easier to liquefy frozen and thawed sand, while decreasing small pore sizes will inhibit liquefaction. However, the effect of decreasing grain sizes and increasing large pore sizes is more obvious, and it is generally easier to liquefy Nanjing sand subjected to freezing and thawing.

7. Conclusions

(1) Under either seismic load or metro train vibration load, freeze-thaw cycles will significantly impair the stiffness and liquefaction resistance of Nanjing sand, especially the first cycle, making Nanjing sand more prone to plastic deformation, and increase the sensitivity of its dynamic pore pressure in response to dynamic load.

(2) The number of freeze-thaw cycles, freezing temperature and effective confining pressure will all affect the liquefaction characteristics of frozen and thawed sand. The more freeze-thaw cycles, the lower the freezing temperature, the smaller the effective confining pressure, the worse the structure of frozen and thawed silty-fine sand, and the easier the liquefaction occurs.

(3) The artificial formation freezing method will harm the liquefaction strength of Nanjing sand, but seismic load poses a small potential risk to Nanjing sand freezing construction.

(4) The vibration of metro trains is a potential liquefaction cause of Nanjing sand. The artificial formation freezing method aggravates the liquefaction potential of Nanjing sand under metro train vibration load, and high-frequency vibration makes it still higher. During freezing construction, liquefaction evaluation and treatment shall be carried out for Nanjing sand each time after freezing, and all efforts shall be made to keep the drainage channel unblocked.

(5) Freeze-thaw cycles will reduce the grain size of Nanjing sand, increase the size of large pores and decrease the size of small pores, and the more freeze-thaw cycles, the more obvious it is.

References

Chen, W., Sun, M., Liu, M., Hu, X., & Zeng, G. (2003). Characters of schistose structure of nanjing's sand and seismic liquefaction of subsoil of a metro section. *Rock and Soil Mechanics*, *24*(5), 755–758, (in Chinese).

Cheng, P., Wang, Y., & Li, X. (2016). Factors and homogeneity of triaxial sand specimens preparation with air pluviation. *Journal of Yangtze River Scientific Research Institute*, *33*(10), 79–83, 92 (in Chinese).

Coal Industry Coal Mine Special Equipment Standardization Technical Committee (2011). *MT/T 593.2—2011 artificial frozen soil physics mechanics performance test*. Beijing: State Administration of Work Safety. (in Chinese).

He, F., Wang, X., Liu, D., Jiang, D., & Liu, B. (2017). Experimental study on dynamic characteristic parameters of undisturbed frozen sandy soil of qinghai-tibet Railway. *Journal of the China Railway Society*, *39*(6), 112–117, (in Chinese).

Hu, Z., Wang, R., Zhuang, H., & Chen, G. (2016). Apparent kinetic viscosity of saturated nanjing sand due to liquefaction-induced large deformation in torsional shear tests. *Chinese Journal of Geotechnical Engineering*, *38*(Supplement 2), 149–154, (in Chinese).

Huang, Y. (2001). Liquefaction of the nanjing sand and its identification. *World Information on Earthquake Engineering*, *17*(1), 69–74, (in Chinese).

Johnson, T. C., Cole, D. M., & Chamberlain, E. J. (1979). Effect of freeze-thaw cycles on resilient properties of fine-grained soils. *Engineering Geology*, *13*(1/2/3/4), 247–276.

Lagioia, R., Sanzeni, A., & Colleselli, F. (2006). Air, water and vacuum pluviation of sand specimens for the triaxial apparatus. *Soils and Foundations*, *46*(1), 61–67.

Li, J. C., Baladi, G. Y., & Andersland, O. B. (1979). Cyclic triaxial tests on frozen sand. *Engineering Geology*, *13*(1/2/3/4), 233–246.

Ma, W., Chen, G., Li, L. E., Wu, Q., & Liu, J. (2019). Experimental study on liquefaction characteristics of saturated coral sand in nansha islands under cyclic loading. *Chinese Journal of Geotechnical Engineering*, *41*(5), 981–988, (in Chinese).

Mei, Y., Zhao, L., Zhou, D., Liu, J., & Zhu, J. (2020). Application of AGF in underground excavation construction of water-rich sand layer. *China Railway Science*, *41*(4), 1–10, (in Chinese).

Sun, J., Gong, M., Xiong, H., & Gan, L. (2020). Experimental study of the effect of freeze-thaw cycles on dynamic characteristics of silty sand. *Rock and Soil Mechanics*, *41*(3), 747–754, (in Chinese).

Tang, Y., Li, J., & Li, J. (2019). Experimental study on dynamic cumulative axial strain performance of artificial frost-thawed saturated silty sand. *Journal of Harbin Institute of Technology*, *51*(2), 76–83, (in Chinese).

Wang, J., Wang, L., & Li, L. (2004). The dynamic triaxial test discrimination and evaluation for liquefaction of saturated sand. *Northwestern Seismological Journal*, *26*(3), 285–288, (in Chinese).

Wang, P., Xu, J., Liu, S., Wang, H., & Liu, S. (2016). Static and dynamic mechanical properties of sedimentary rock after freeze-thaw or thermal shock weathering. *Engineering Geology*, *210*, 148–157.

Wang, T., Wang, H., Song, H., Wang, O., & Liu, J. (2019). Evolution laws of mechanical properties of artificially frozen silty clay. *China Railway Science*, *40*(1), 1–7, (in Chinese).

Yan, H., Wang, T., Liu, J., & Wang, Y. (2014). Experimental study of dynamic parameters of silty soil subjected to repeated freeze-thaw. *Rock and Soil Mechanics*, *35*(3), 683–688, (in Chinese).

Zhang, Y. (2016). Analysis of measured vibration wave on the top of subway tunnel. *Journal of Engineering Technology*, *3*, 286, (in Chinese).

Corresponding author
Zeyao Li can be contacted at: lzy004@tongji.edu.cn